JOURNAL OF MATERIALS SCIENCE **38** (2003) 713–720

Mechanism of Fe-Mn-Al alloy steel ingot failure from MgO-C refractory corrosion

JYH-WEI LEE*
Department of Mechanical Engineering, Tung Nan Institute of Technology, Taipei, Taiwan
E-mail: jefflee@mail.me.tnit.edu.tw

JENQ-GONG DUH
Department of Materials Science and Engineering, National Tsing Hua University, Hsinchu, Taiwan

Fe-Mn-Al alloy steel was melted in a mass production tonnage arc furnace equipped with ladle refining facilities. The ingots were cracked and torn apart on hot rolling. Blue flames erupted from the cracks and became red. A white powder was observed adjacent to the cracks in ingots. The white powder was identified as magnesia. Concentrations of Mg and Ca were high in the centre of the ingot, implying the segregation of impurities. Quantitative elemental analysis and microstructural investigation revealed Mg, Si, Ca and S containing impurities and Cr, Mo and Si carbides were segregated within grain boundaries. The segregation was the main cause of ingot cracking. The 1600°C static cup test for carbon containing MgO-C refractories exhibited the reduction reaction, which raised the Mg concentration up to 0.017 wt% in Fe-Mn-Al alloy steel, whereas the pure MgO refractory cup test showed inertness to Fe-Mn-Al alloy.

1. Introduction

The melting process in the steel making industry is laborious and complex. Secondary refining has been employed to achieve high quality for special alloy steels, such as tool steels and stainless steels. The arc furnace is used to melt the steel first, and a ladle or other induction furnace is used for refining, which can include deoxidization, desulfurization, decarburization, slagmaking, composition adjustment, argon stirring, low pressure or vacuum degassing and calcium powder injection. One of the major controlling factors that affects the quality of steel melts during secondary refining is the lining of the furnace. This is constructed from refractories, which should be capable of containing molten metal at temperature exceeding 1500°C. The lining refractories should maintain inertness and have no interaction with steel melts or slag. The proper choice of lining refractories will ensure longer service life, lower cost and good quality steel products.

Aluminium exhibits high activity and tends to be oxidized easily. Usually aluminium is employed as an oxygen removal agent, and added in very small amounts, as little as 0.03 wt% to the steel during melting. The added aluminium will be oxidized and float as slag on the surface of the steel melts. Only small amounts of alumina, around 0.015 to 0.02 wt%, will remain in the liquid steel and become inclusions as a steel solidifies. The role of aluminium as a grain refining agent was discussed by Deeley [1], but the addition of aluminium as an alloying element in conventional steel is rare. These are only a limited number of steels with aluminium contents higher than one percent that are used in the steel industry. Thus, the reactions between aluminium and refractories in steel making have seldom been discussed in the literature. Sharp [2] revealed that the nozzle was easily blocked by alumina when teeming aluminium-killed steel. The reduction reaction of SiO_2 in aluminosilicate refractory by aluminium [in aluminium processing] was recently reported by Lee [3].

Fe-Mn-Al alloy steels have aluminium contents higher than 7 wt% with Fe-30 wt% Mn-9 wt% Al-1 wt% C being a typical composition. Hadfield [4] invented this alloy in 1887. The claimed chemical composition was Fe- (0.1–30%)Mn- (0.1–20%)Al- (0.1–6%)Si -(0.1–3%)C. The shortage of nickel during the Korean War made the industry stress the develop low nickel or no nickel stainless steels. The nickel-free Fe-Mn-Al alloy steel was thus of interest [5, 6]. At that time, the major research topic concerning this alloy was high temperature oxidation and sulfidation. Some researchers tried to use Fe-Mn-Al alloy as a substitute for conventional Fe-Ni-Cr stainless steels, in which manganese substituted for nickel, and chromium was replaced by aluminium [5]. Over the past decades, Fe-Mn-Al alloys have been studied widely around the world. The high temperature oxidation behavior [7, 8], oxidation induced phase transformation phenomena [9] and hot corrosion resistance [10] of Fe-Mn-Al-C alloys have been studied. The Famcy Steel Corp. in Pittsburgh,

*Author to whom all correspondence should be addressed.

USA developed the mass production process for this alloy during the 1990's [11–13]. The purpose of this study is to investigate the reactions between refractory materials and steel melts in the mass production process. Microstructural evaluation of the ingot, especially the observation of macrocracks in the broken ingot, will be further discussed.

2. Experimental procedure

A mass production scale melting process was employed in this study. The scrap, ferromanganese and ferrochromium were first melted in an arc furnace. After melting, the liquid steel was then tapped into a ladle containing aluminium. The aluminium was melted and stirred by the flushing and circulation of liquid steel from the arc furnace. The ladle was further moved to the refining furnace station to adjust chemical composition and temperature and then proceeded to the slag making station. The desulfurization process took place at the injection station.

After the refining processes, the liquid steel was teemed to steel molds with argon shrouding. The dimensions of steel ingots were 660 mm × 890 mm × 1854 mm, and each weighed about 5200 kilograms. Ingots were annealed at 1100°C for more than 8 hours, hot rolled to hot bands and then cold rolled to strips with conventional hot and cold rolling machines for 304 stainless steels. The cracking failure of the ingots occurred in the hot rolling process. This occurred from the early development stage of the process at the Famcy Steel Corp. Ingots were cracked and torn apart on hot rolling between 1204 and 1093°C. Blue flames which turned red erupted from the cracks. A white powder was observed beside the cracks after the ingots cooled to room temperature as shown in Fig. 1a–c.

The white powder beside the cracks in the ingots was collected and analyzed by X-ray diffractometry. The chemical composition of charged alloying materials including scrap, ferromanganese, ferrochromium, ferromolybdenum, ferroaluminium and pure aluminium

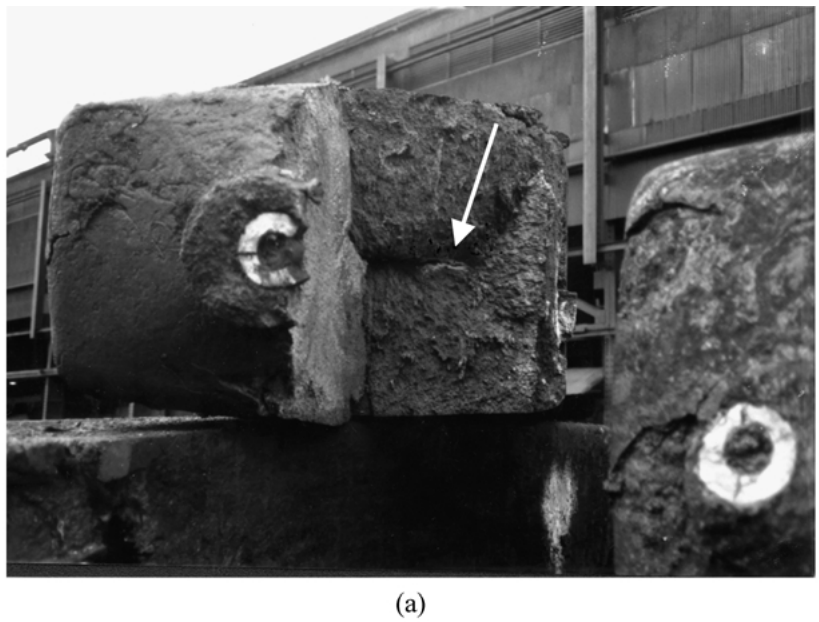

(a)

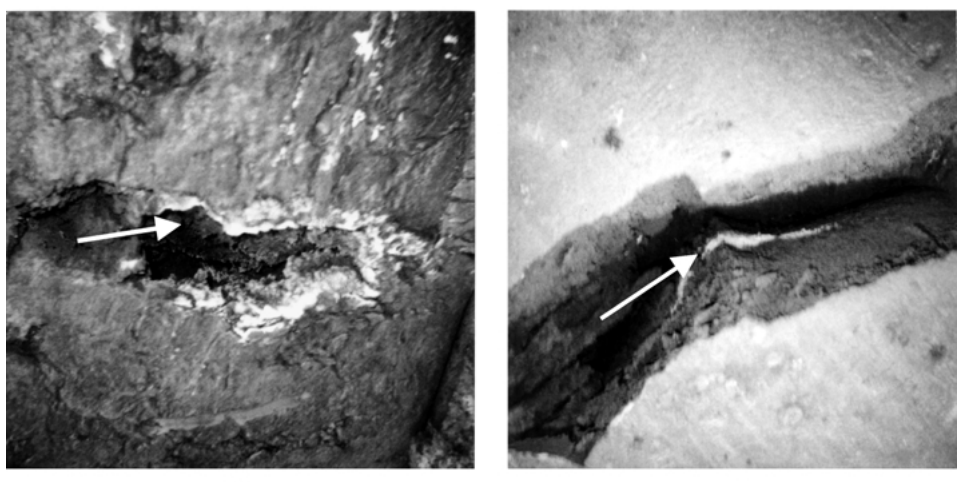

(b) (c)

Figure 1 Micrographs of a broken ingot in (a) the bottom portion, the white powder observed in the shrinkage pipe of the ingot, (b) the side view and (c) the top view of the broken ingot with white powder adjacent to the crack.

were analyzed by Induction Coupled Plasma (ICP) spectroscopy and Atomic Absorption Spectrometry (AAS). Samples from the 1800 kilograms of CaO flux, 270 kilograms of CaO, 27 kilograms of CaF synthetic slag, 150 Kilograms of CaO and 50 kilograms of CaSi injection powders were also analyzed by energy dispersive X-ray spectroscopy in the scanning electron microscopy (SEM-EDS) to check if any other impurity existed.

The broken ingot specimen, the chemistry analysis sample taken during melting and the runner specimen were analyzed by ICP, AAS, wet chemical methods and Leco CS analyzer to identify the chemical composition variation of the ingot. The same Fe-Mn-Al alloy ingot, which had not been hot rolled, was cut vertically in half and then cut horizontally into four pieces from the centre with a high speed steel saw. Five specimens were taken, ranging from the centre of the ingot to the surface, at 100 mm intervals. These five specimens were also analyzed to identify the chemical segregation within the ingot.

The broken pieces of the ingots were cut, ground and polished, using 0.05 μm alumina powder. The morphologies of specimens were examined with an optical microscope and a scanning electron microscope. The elemental distributions in the specimens were dectected by an Electron Probe Microanalyzer (EPMA, JEOL JXA-8800M).

MgO-C (78 wt% MgO-18 wt% C) and MgO (98 wt% MgO-1.1wt% CaO-0.2 wt%Al_2O_3-0.7 wt% SiO_2-0.4 wt% Fe_2O_3) refractories were used as the slag line and the wall lining bricks in the ladle furnace in the Fe-Mn-Al alloy steel melting practice. In order to examine the influence of refractories on the steel melt, verification cup tests for MgO-C and high MgO refractories were conducted. Refractory bricks were cut into $150 \times 150 \times 130$ mm hexahedrons. One of the 150×150 mm surfaces was then drilled with a hole of diameter 35 mm and 40 mm in depth. A similar chemistry Fe-Mn-Al alloy specimen was employed to conduct the high temperature reaction test. The static cup test alloy specimen was made in the 30 Kg induction furnace with electric manganese, 1008 carbon steel, pure aluminium, fereochromium and ferromolybdenum. The alloy was hot forged at 1100°C and then machined into the dimensions of the hole. The test specimen was held at 1600°C for 1 hour and then air cooled.

3. Results

3.1. White powder and charged raw materials analysis

The crystalline phase of the white powder adjacent to the cracks of the ingots was analyzed by X-ray diffractometry and identified as pure magnesia. The chemical compositions of the charged raw materials are listed in Table I. It appears that the "pure" aluminium contained 0.25 wt% Mg. The flux, synthetic slag and injection powders were also analyzed by SEM-EDS. However, no magnesium containing impurity was found.

TABLE I Chemical analysis of alloying materials (wt%) obtained by ICP

	Composition					
Alloying materials	Mn	C	P	S	Si	Others
High carbon ferromanganese	76.1	7.02	0.078	0.011	0.03	Fe balanced
Low carbon ferrochromium	–	0.05	0.024	0.003	0.5	71%Cr, Fe balanced
Pure aluminium	–	–	0.005	–	1.7	0.25%Mg[a], 3.6%SiO_2, Al balanced
Ferromolybdenum	–	0.03	0.046	0.03	0.5	65%Mo, Fe balanced
Steel scrap	0.45	0.2	0.01	0.015	0.01	0.02%Cr, 0.01%Mo, Fe balanced
Ferroaluminium	–	0.08	0.014	0.007	0.14	35.5%Al, Fe balanced

[a]Mg analyzed by AAS.

TABLE II Chemical analysis (wt%) of the Fe-Mn-Al ingot

	Composition										
Specimen	Al	Mo	Cr	Ca	Mn	Si[a]	Mg[b]	C[c]	P[a]	S[c]	Fe
Melt specimen	6.98	2.30	6.13	0.023	29.2	0.330	0.015	0.99	0.029	<0.03	Bal.
Runner specimen	6.87	2.25	6.14	0.062	29.4	0.335	0.023	1.04	0.024	<0.03	Bal.
Broken ingot specimen	6.81	2.27	5.97	0.025	28.9	0.361	0.018	1.01	0.022	<0.03	Bal.
Specimen from the centre of the cut ingot	6.81	2.31	5.89	0.034	28.3	0.342	0.018	0.99	<0.003	–	Bal.
Specimen 100 mm away from the centre of the cut ingot	6.80	2.22	5.86	0.017	28.3	0.348	0.016	0.97	<0.003	–	Bal.
Specimen 200 mm away from the centre of the cut ingot	6.94	2.27	5.80	0.016	28.5	0.350	0.016	0.98	<0.003	–	Bal.
Specimen 300 mm away from the centre of the cut ingot	6.52	2.28	6.11	0.019	27.5	0.352	0.016	1.08	<0.003	–	Bal.
Specimen from the surface of the cut ingot	6.86	2.25	5.85	0.018	28.3	0.356	0.016	0.97	<0.003	–	Bal.
The average of the cut ingot	6.79	2.22	5.91	0.022	28.3	0.352	0.0167	1.00	–	<0.03	Bal.

[a]Si, P analyzed by wet chemical.
[b]Mg analyzed by Flame AAS.
[c]C, S analyzed by Leco CS analyzer.
[d]Other alloy elements analyzed by ICP.

3.2. Chemical composition analysis of the ingots

The chemical compositions of the broken ingot specimen, the sample taken from the melt, the runner specimen and five specimens from the unrolled ingot are listed in Table II. It is apparent that the concentrations of major elements, such as manganese, aluminium, chrominum, molybdenum and carbon exhibit little deviation from the centre to the surface of the cut ingot. This observation is also valid for the melt specimen, runner specimen and broken ingot specimen. However, the amounts of magnesium and calcium increase dramatically near the centre of the ingot. Higher levels of these two elements are also found in the runner specimen. It is noticeable that the concentration of magnesium in the broken ingot specimen was also appreciable.

3.3. Microstructural analysis of the ingot

Optical micrographs of the broken pieces of the ingot are shown in Fig. 2. Radial microcracks from the grain boundaries are obvious in Fig. 2a. Island–like phases and elliptical precipitates are visible along the grain boundaries. A macrocrack propagates along the grain boundary, as seen in Fig. 2b, while the white precipitate adjacent to the macrocrack is evident.

Secondary electron images and X-ray maps for the grain boundary and precipitates are shown in Figs 3 and 4. On the basis of the images and X-ray map results of the grain boundary in Fig. 3, it is believed that the grain boundary appears as a deep fissure. Some particle-like phases have segregated to the boundary; these are magnesium, silicon, calcium, sulfur and oxygen rich. The oxides of Mg, Si , Ca and S, segregated within the grain boundary, are the last to solidify. A half elliptical precipitate is observed at the intersection of several grains in Fig. 4a. There are lots of small holes around the precipitate, which are lined up radially. X-ray mapping leads to the identification of this precipitate as a Cr, Mo and Si rich carbide. In addition, an overview of microcracks in the broken ingot is indicated in Fig. 5. Together with the corresponding X-ray maps for Mg, Cr, Mo, O, Si and C.

3.4. Verification cup tests of refractories

Fig. 6 shows the cross-sectional view of the MgO-C and the high MgO refractory cups after the 1600°C static test for 1 hour. The chemical compositions of the Fe-Mn-Al alloy specimens before and after cup tests are listed in Table III. It is clear that more extensive interaction has taken place in the MgO-C test than in the MgO test. There is no significant variation in the chemical compositions of the major elements, except aluminium which changed dramatically in the MgO-C cup test. Silicon increases in the two Fe-Mn-Al alloy specimens after the two cup tests, whereas the composition of magnesium is high only for the specimen tested in the MgO-C refractory cup.

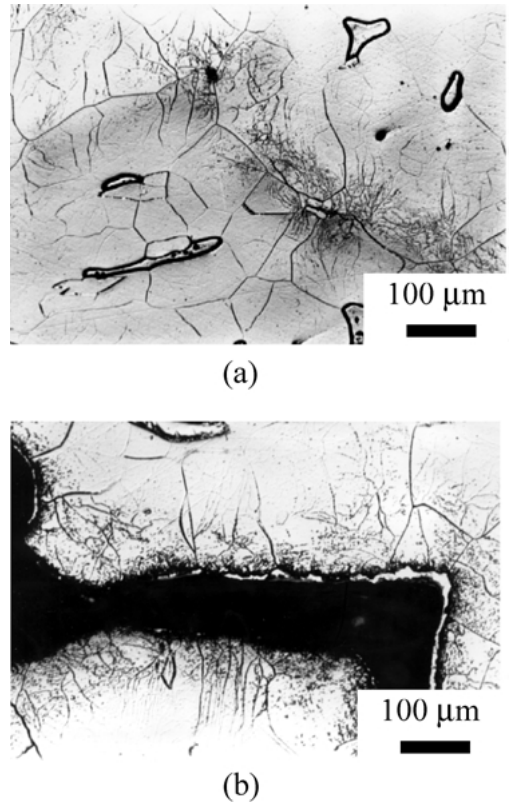

Figure 2 Optical micrographs of (a) island-like phases, elliptical precipitates and radial microcracks in grain boundaries and (b) macro and microcracks of the broken ingot.

4. Discussion

4.1. Inclusion segregation, precipitation and crack initiation

Figs 2 to 4 and the chemical composition analysis across the ingot reported in Table II reveal some

TABLE III Chemical compositions of Fe-Mn-Al alloys (wt%) in cup tests

Samples	Composition							
	Al	Mo	Cr	Ca	Mn	Si[a]	Mg[b]	Fe
Before Cup Test	7.55	1.72	6.17	<0.02	26.2	<0.025	<0.01	Bal.
MgO Cup, 1600°C (1 hr)	6.52	1.76	6.33	<0.02	26.0	0.103	<0.01	Bal.
MgO-C Cup, 1600°C (1 hr)	2.35	1.81	6.43	0.02	26.4	0.125	0.017	Bal.

[a]Si analyzed by wet chemical.
[b]Mg analyzed by Flame AAS.

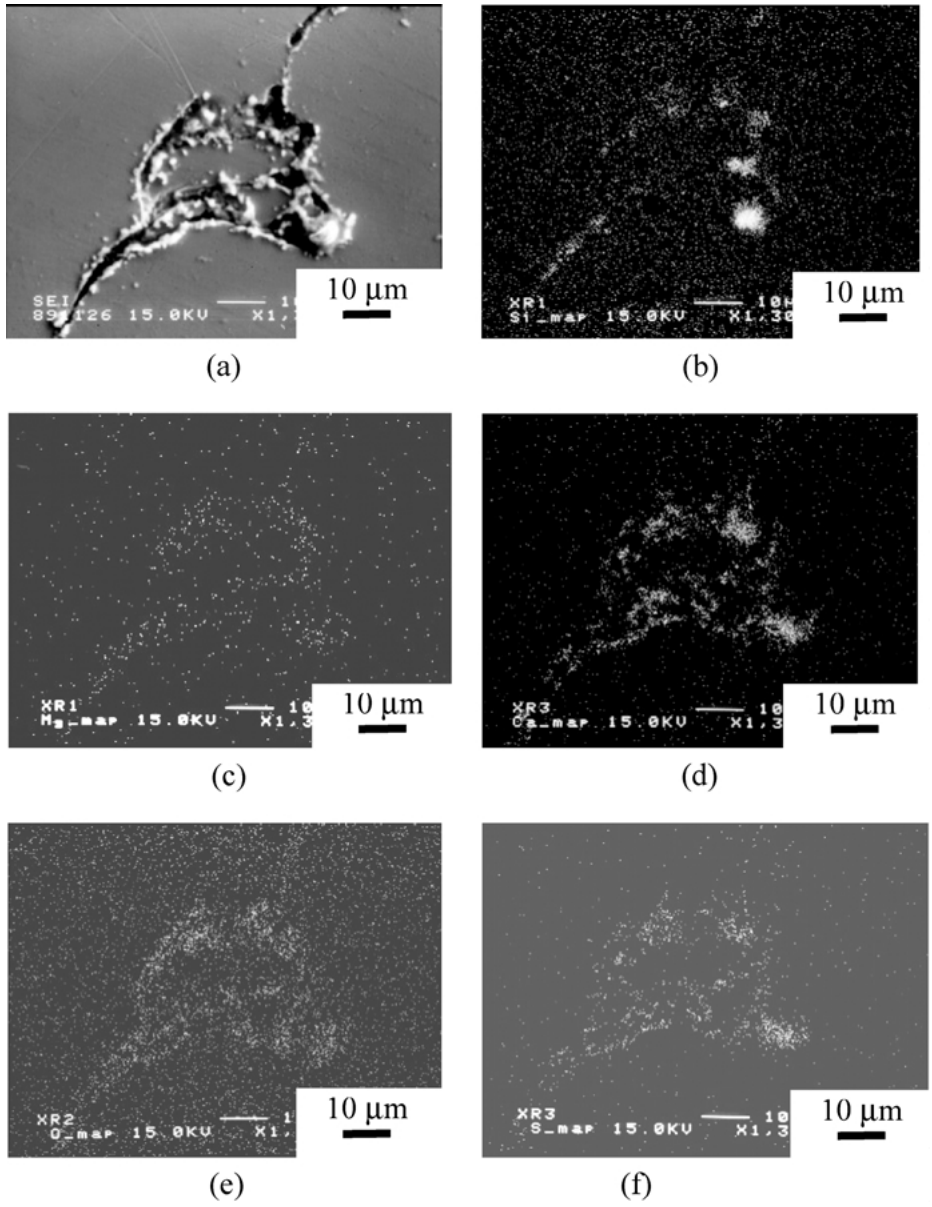

Figure 3 Inclusions in the grain boundary of the broken ingot. (a) Scanning electron micrograph, (b) Si X-ray map, (c) Mg X-ray, (d) Ca X-ray map, (e) O X-ray map and (f) S X-ray map.

important features. Mg, Ca, Si and S were trapped as the oxide forms in grain boundaries. In addition, carbide precipitation along the grain boundary was observed. The region of inclusions should be the origin of cracking on hot rolling. Macrocracks which had propagated along the grain boundaries are observed (Fig. 5a). The precipitate in grain boundaries is torn apart by the macrocracks (Fig. 5b) found X-ray maps reveal that Cr, Mo, Si and C are rich in the precipitate, whereas Mg, Si and O are found in the crack. Such results are in agreement with the observations in Figs 3 and 4. Major cracks in Fig. 2 are all intergranular, whereas microcracks are radial from major cracks. A cast ingot which cracked during forging was reported by Naumann [14]. The intergranular or primary grain boundary fracture failure was caused by the precipitation of AlN, as well as other hard-to-dissolve phases, such as oxides,carbides and sulfides. Hilty revealed that the mechanical behavior of steel is controlled mainly by the volume fraction, size distribution, composition and morphology of inclusions and precipitates [15]. Inclusions with size greater than 1 μm have deleterious effects on steel ductility and toughness. In this study, the precipitates are usually larger than 1 μm, with some larger than 5 μm. In addition, impurities are all concentrated on grain boundaries. Thus, the cracking of Fe-Mn-Al alloy during hot rolling results.

4.2. Interaction of MgO refractory materials and Fe-Mn-Al alloy

Magnesia is the most important refractory used in basic slag steelmaking practice. The carbon (mainly graphite) containing MgO-C refractory shows excellent thermal shock resistance and crack-propagation-resistance [3, 16–18]. The magnesia-carbon reaction in this refractory material has been studied for years [3, 16, 17,

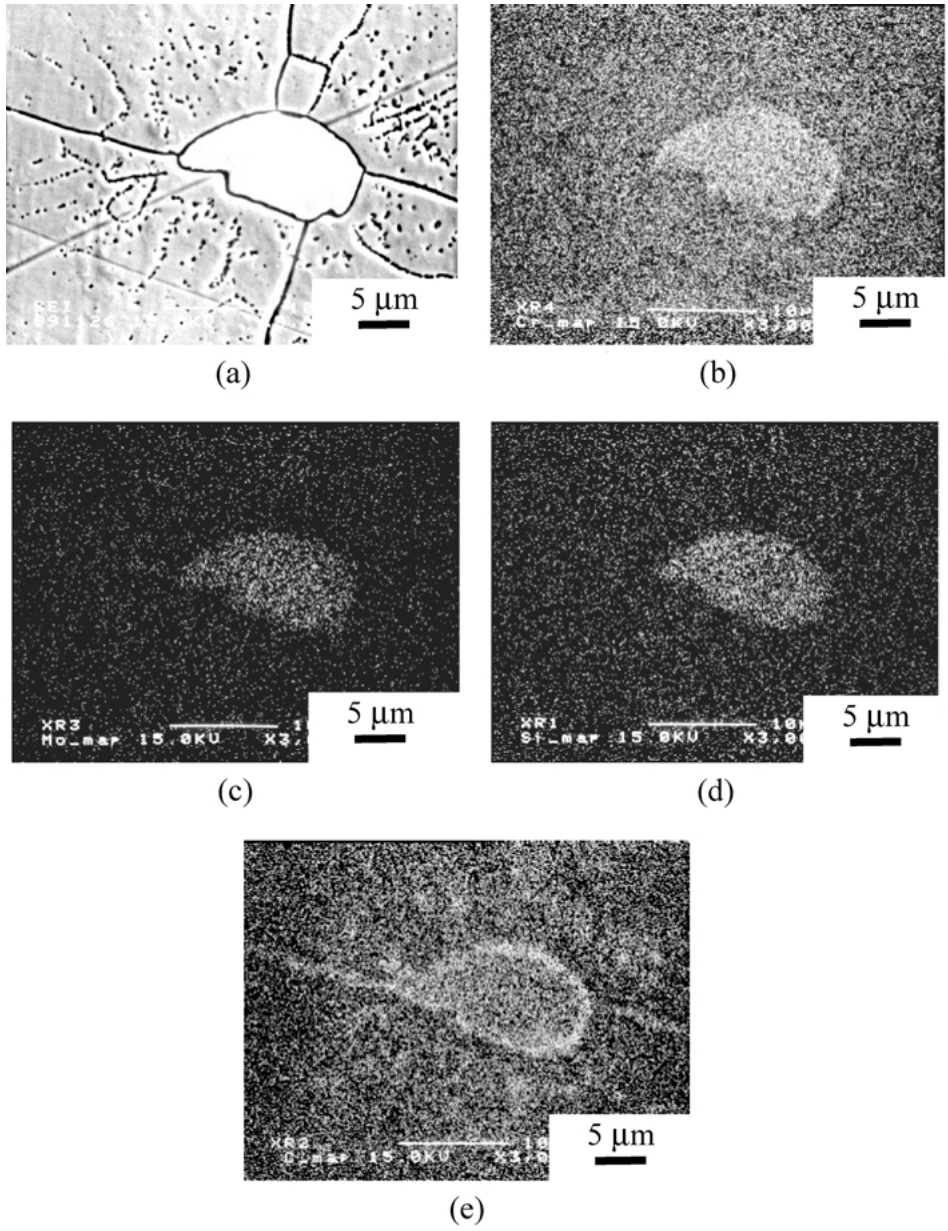

Figure 4 Precipitate in grain boundary of the broken ingot. (a) Scanning electron micrograph, (b) Cr X-ray map, (c) Mo X-ray map, (d) Si X-ray map and (e) C X-ray map.

19–23]. The basic reaction is:

$$\begin{gathered} \mathrm{MgO(s)} + \underline{\mathrm{C}}\mathrm{(s)} = \mathrm{Mg(g)} + \mathrm{CO(g)} \\ \Delta G^\circ = 146550 - 69.25T \end{gathered} \tag{1}$$

The data from the MgO-C cup test indicates that the aluminium content dropped to only 2.35 wt%, whereas the magnesium content rose to 0.017 wt%. It appears that the carbon containing MgO-C refractory is reduced by the aluminium in the alloy. Possible reactions are listed as follows [24]:

$$\begin{gathered} 2\mathrm{Al(l)} + 3/2\mathrm{O_2(g)} = \mathrm{Al_2O_3(s)} \\ \Delta G^\circ = -402300 + 77.83T \end{gathered} \tag{2}$$

$$\begin{gathered} \mathrm{MgO(s)} = \mathrm{Mg(g)} + 1/2\mathrm{O_2(g)} \\ \Delta G^\circ = 176060 - 49.84T \end{gathered} \tag{3}$$

$$\begin{gathered} 2\mathrm{Al(l)} + 3\mathrm{MgO(s)} = 3\mathrm{Mg(g)} + \mathrm{Al_2O_3(s)} \\ \Delta G^\circ = 125880 - 71.69T \end{gathered} \tag{4}$$

From thermodynamic calculations, the equilibrium of Equation 4 can be achieved at 1483°C when the magnesium partial pressure is 1 atm. Magnesium is essentially insoluble in the solid steel and is normally added to the cast iron as an inoculant. It is also used as a desulfurizer in steelmaking. The solubility of magnesium in liquid steel at 1600°C is about 1 wt% [25], and the addition of C, Ni and Al in the steel will increase the solubility of magnesium in liquid steel. In this study, the solubility of magnesium in the Fe-Mn-Al alloy steel at room temperature is around 0.017–0.018 wt%.

From the data from the cup tests of Fe-Mn-Al alloy steel, the MgO brick is inert to the liquid steel, while the MgO-C refractory materials should be avoided in

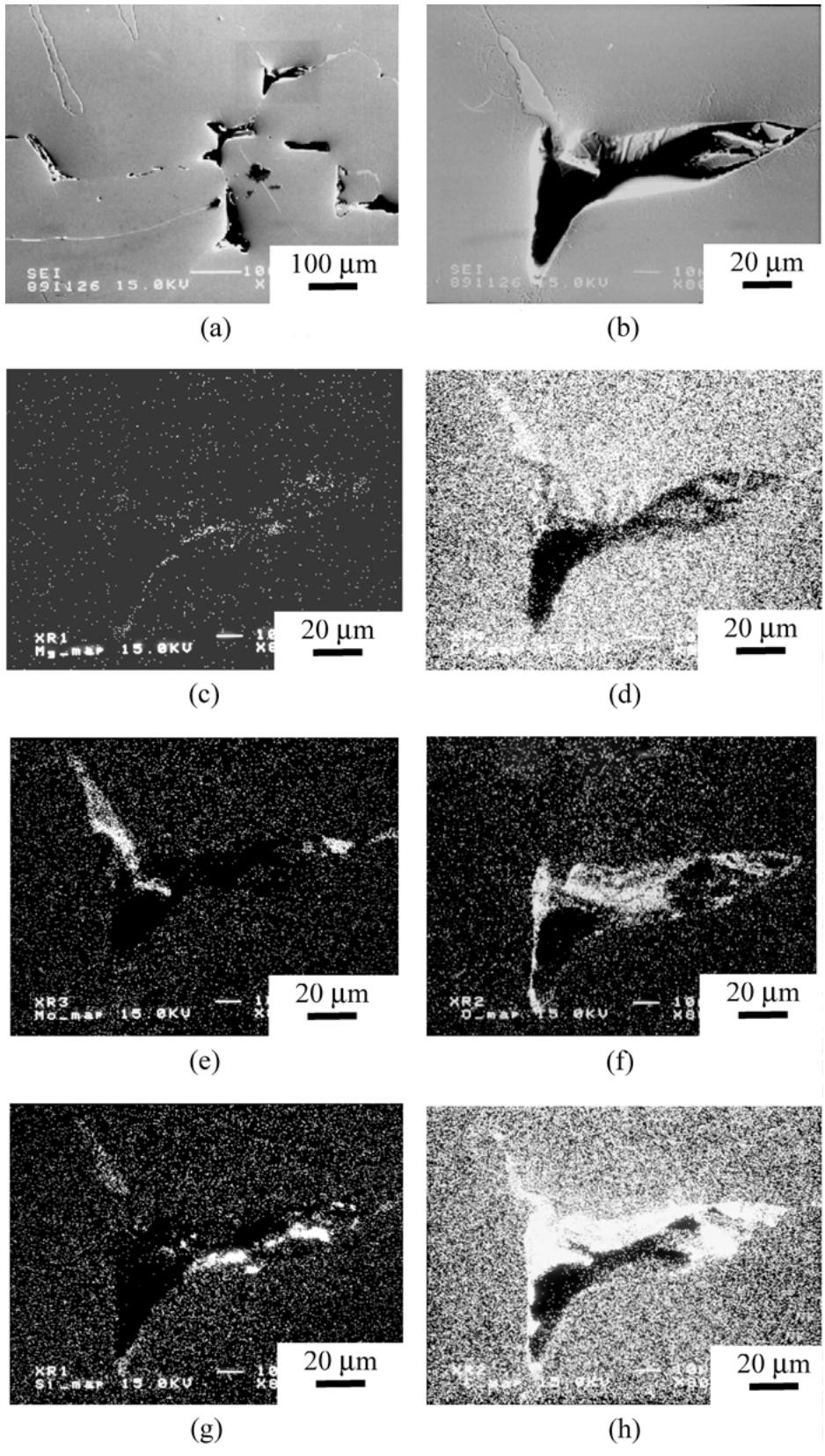

Figure 5 (a) An overview of microcracks in the broken ingot. (b) The microcrack at higher magnification and X-ray maps of (c) Mg, (d) Cr, (e) Mo, (f) O, (g) Si and (h) C.

the melting practice. According to Equation 4 and the results of cup tests, the magnesia in MgO-C refractory materials was reduced to magnesium which dissolved in the steel. This could occur in the melting of Fe-Mn-Al alloy steel in the ladle furnace. Due to the decrease of Mg solubility when the steel solidified, the excess Mg was ejected and oxidized to magnesia. Magnesia was trapped as impurities in shrinkage pipes and grain boundaries as seen in Figs 3 and 5.

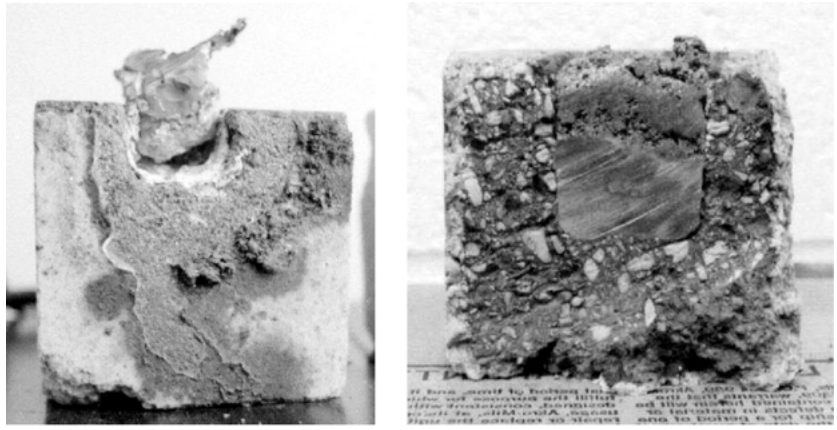

Figure 6 The cross-sectional morphologies of the (a) MgO-C brick and (b) MgO brick after 1600°C static cup tests for 1 hour.

5. Conclusions

1. The Fe-28Mn-7Al-6Cr-1C-2.2Mo-0.33Si alloy was melted with a mass production scale arc furnace followed by ladle refining. Failure occurred during hot rolling of ingots.

2. A white powder later identified as magnesia was observed adjacent to the crack after the ingot cooled to room temperature. Detailed observations revealed that inclusions containing Mg, Si, Ca, S and O were segregated within grain boundaries. Cr, Mo and Si rich carbides were also visible in the grain boundaries.

3. Magnesium and calcium concentrations were high in the centre of the ingot, indicating the segregation of impurities. Cracks were initiated from grain boundaries filled with impurities and precipitates.

4. Static cup testing of Fe-Mn-Al alloy in MgO-C refractory materials showed the reduction of magnesia by aluminium in the reducing atmosphere caused by carbon. The pure MgO refractory, without carbon, exhibited no deleterious effect on the alloy.

5. Some portions of MgO-C slag line refractory bricks were reduced to magnesium by aluminium and dissolved in the high temperature liquid Fe-Mn-Al alloy steel during the ladle refining process. The excess magnesium was ejected and oxidized to magnesia when alloy steel solidified. Magnesia was trapped as impurities in shrinkage pipes and grain boundaries in Fe-Mn-Al alloy steel ingots.

Acknowledgements

The authors would like to thank S.J. Chen , C.D. Chiang and The Famcy Steel Corp. for their contributions to this study. The financial support of NSC of Rep. of China, Taiwan through contract No. NSC-89-2216-E-236-001 is also greatly appreciated.

References

1. P. D. DEELEY, K. J. A. KUNDIG and H. R. SPENDELOW Jr., in "Ferroalloys & Alloying Additives Handbook" (Shieldalloy Corp. Newfield, NJ, Metallurgy Alloy Corp, New York, 1981) p. 1.
2. J. D. SHARP, in "Small-Scale Steelmaking," edited by R. D. Walker (Applied Science Publishers, Essex, England, 1983) p. 89.
3. W. E. LEE, *J. Amer. Ceram. Soc.* **81**(6) (1998) 1385.
4. R. A. HADFIELD, US Patent 422403 (1887).
5. J. R. MITCHELL and M. E. POTTER, US Patent 3201230 (1965).
6. J. L. HAM and R. Z. CARINS, *Product Engineering* **52** (1958) 29.
7. C. J. WANG and J. G. DUH, *J. Mater. Sci.* **23** (1988) 769.
8. C. J. WANG, J. W. LEE and J. G. DUH, *ibid.* **23** (1988) 2649.
9. J. G. DUH and J. W. LEE, *J. Electrochem. Soc.* **136**(3) (1989) 847.
10. C. J. WANG, J. W. LEE and C. H. KAO, in Proc. 9th Asian-Pacific Corrosion Control Conference, Vol. 1, edited by S. L. I. Chan and W. T. Tsai (Corrosion Engineering Association of the R.O.C., Taipei, Taiwan, 1995) p. 141.
11. C. M. WAN, US Patent 4975335 (1990).
12. *Idem.*, US Patent 4875933 (1990).
13. *Idem.*, Australia Patent 610429 (1990).
14. F. K. NAUMANN and F. SPIES, in "Failure Analysis" (Riederer-Verlag, Stuttgart, Germany/American Society for Metals, Metals Park, OH, 1983) p. 112.
15. D. C. HILTY, in "Electric Furnace Steelmaking," edited by C. R. Taylor and C. C. Custer (The Iron and Steel Society, 1985) p. 238.
16. C. BAUDIN, C. ALVAREZ and R. E. MOORE, *J. Amer. Ceram. Soc.* **82**(12) (1999) 3529.
17. *Idem.*, *ibid.* **82**(12) (1999) 3539.
18. C. F. COOPER, I. C. ALEXANDER and C. J. HAMPSON, *Br. Ceram. Trans. J.* **84** (1985) 57.
19. P. L. SMITH, J. LIDDLE and J. WHITE, *ibid.* **84** (1985) 62.
20. B. BREZNY, *J. Amer. Ceram. Soc.* **59**(11/12) (1976) 529.
21. S. C. CARNIGLIA, *Ceramic Bulletin* **52**(2) (1973) 160.
22. R. J. LEONARD and R. H. HERRON, *J. Amer. Ceram. Soc.* **55**(1) (1972) 1.
23. J. F. ELLIOTT, in "Electric Furnace Steelmaking," edited by C. R. Taylor and C. C. Custer (The Iron and Steel Society, 1985) p. 312.
24. H. E. McGANNON, in "The Making, Shaping and Treating of Steel," edited by H. E. McGannon (United States Steel, Pittsburgh, PA, 1970) p. 297.
25. K. W. LANGE, *Int. Mater. Rev.* **33**(2) (1988) 53.

Received 9 April
and accepted 2 October 2002